



Effects of cylindrospermopsin, chlorpyrifos and their combination in a SH-SY5Y cell model concerning developmental neurotoxicity

M.G. Hinojosa^{a,b}, Y. Johansson^{a,*}, A. Jos^b, A.M. Cameán^b, A. Forsby^a

^a Department of Biochemistry and Biophysics, Stockholm University, 106 91 Stockholm, Sweden

^b Area of Toxicology, Department of Nutrition and Bromatology, Toxicology and Legal Medicine. Faculty of Pharmacy, University of Seville, C/ Profesor García González 2, 41012 Seville, Spain

ARTICLE INFO

Editor: Professor Bing Yan

Keywords:

Cylindrospermopsin
Chlorpyrifos
Developmental neurotoxicity
Neurite outgrowth
nAChRs
Transcriptomics

ABSTRACT

The cyanotoxin cylindrospermopsin (CYN) has been postulated to cause neurotoxicity, although the studies in this concern are very few. In addition, some studies in vitro indicate its possible effects on development. Furthermore, pesticides can be present in the same environmental samples as cyanotoxins. Therefore, chlorpyrifos (CPF) has been one of the most common pesticides used worldwide. The aim of this report was to study the effects of CYN, isolated and in combination with CPF, in a developmental neurotoxicity in vitro model. The human neuroblastoma SH-SY5Y cell line was exposed during 6 days of differentiation to both toxics to study their effects on cell viability and neurite outgrowth. To further evaluate effects of both toxicants on cholinergic signaling, their agonistic and antagonistic activities on the $\alpha 7$ homomeric nicotinic acetylcholine receptor (nAChR) were studied upon acute exposure. Moreover, a transcriptomic analysis by qPCR was performed after 6 days of CYN-exposure during differentiation. The results showed a concentration-dependent decrease on both cell viability and neurite outgrowth for both toxics isolated, leading to effective concentration 20 (EC₂₀) values of 0.35 μ M and 0.097 μ M for CYN on cell viability and neurite outgrowth, respectively, and 100 μ M and 58 μ M for CPF, while the combination demonstrated no significant variations. In addition, 95 μ M and 285 μ M CPF demonstrated to act as an antagonist to nicotine on the nAChR, although CYN up to 2.4 μ M had no effect on the efficacy of these receptors. Additionally, the EC₂₀ for CYN (0.097 μ M) on neurite outgrowth downregulated expression of the 5 genes *NTNG2* (netrin G2), *KCNJ11* (potassium channel), *SLC18A3* (vesicular acetylcholine transporter), *APOE* (apolipoprotein E), and *SEMA6B* (semaphorin 6B), that are all important for neuronal development. Thus, this study points out the importance of studying the effects of CYN in terms of neurotoxicity and developmental neurotoxicity.

1. Introduction

In the last decades, the climate change and the anthropogenic activities have led to undesirable effects on the aquatic environment, causing physical changes in surface water that favor the variation in the present biota (Buratti et al., 2017). Among them, the growth in blooms of cyanobacteria is of especial concern, as their adaptive ability allows them to be found in many environmental samples even under extreme

conditions (Huisman et al., 2018). Although these microorganisms have applications in different industries such as agriculture or cosmetics, many species are also able to produce toxic compounds known as cyanotoxins (Buratti et al., 2017). In this sense, the cytotoxin cylindrospermopsin (CYN) is the second most studied cyanotoxin due to its global distribution, its bioaccumulation and its toxicity (Yang et al., 2021). This small molecule (415 Da) consists of a tricyclic guanidine moiety with a hydroxymethyluracil and a sulfonic acid group. Its

Abbreviations: ACh, acetylcholine; AChE, acetylcholinesterase; APOE, Apolipoprotein E; BBB, blood-brain barrier; [Ca²⁺]_i, intracellular levels of free calcium; ChAT, Choline acetyltransferase; CPF, Chlorpyrifos; CYN, Cylindrospermopsin; DMSO, dimethyl sulfoxide; EC, effective concentration; GSH, glutathione; hiPSCs, human induced pluripotent stem cells; KCNJ11, Potassium Inwardly Rectifying Channel Subfamily J Member 11; mAChRs, muscarinic acetylcholine receptors; MEM, minimum essential medium; nAChRs, nicotinic acetylcholine receptors; NEAA, non-essential amino acids solution; NSCs, neural stem cells; NTNG2, netrin G2; OPs, organophosphates; PenStrep, Penicillin and Streptomycin; PNU-120596, N-(5-Chloro-2,4-dimethoxyphenyl)-N'-(5-methyl-3-isoxazolyl)-urea; RA, all-trans retinoic acid; RT-qPCR, Reverse transcriptase quantitative polymerase chain reaction; SEMA6B, semaphorin 6B; SLC18A3, Solute Carrier Family 18 Member A3.

* Corresponding author.

E-mail address: ylva.johansson@dbb.su.se (Y. Johansson).

<https://doi.org/10.1016/j.ecoenv.2023.115804>

Received 6 September 2023; Received in revised form 5 December 2023; Accepted 6 December 2023

Available online 12 December 2023

0147-6513/© 2023 The Authors. Published by Elsevier Inc. This is an open access article under the CC BY license (<http://creativecommons.org/licenses/by/4.0/>).

zwitterionic properties make this alkaloid a highly water-soluble molecule (Ohtani et al., 1992). The main producing species is *Raphidiopsis raciborskii* (previously known as *Cylindrospermopsis raciborskii*), although some other species such as *Aphanizomenon flos-aquae*, *Chrysochloris ovalisporum*, *Raphidiopsis curvata*, or *Anabaena bergii* among others are also able to produce this cyanotoxin (Manning and Nobles, 2017). Due to this, CYN has caused many human and animal poisoning cases. In this regard, the main case of human poisoning attributed to CYN was the one known as the “mystery disease of Palm Island”, in 1979 in Australia. This illness, which affected around 150 people, could be referred to a drinking water reservoir that contained a bloom of *R. raciborskii* producing CYN, which caused symptoms of gastroenteritis and renal insufficiency (Byth, 1980). Regarding this, although the main organ targets of this toxin are the liver and the kidneys, it has demonstrated to cause effects in many other organs as well such as heart, lungs, and the immune, endocrine, and nervous systems (Buratti et al., 2017; Hinojosa et al., 2019a; Diez-Quijada et al., 2021; Casas-Rodríguez et al., 2022). In general, the main mechanism of action is the protein synthesis inhibition (Terao et al., 1994), including the inhibition of the synthesis of the tripeptide glutathione (GSH) (Runnegar et al., 1995). This inhibition may also result in oxidative stress and apoptosis (Yang et al., 2021). Furthermore, some in vitro studies suggest that CYN may be a possible pro-genotoxic compound, needing the previous activation by the enzymatic complex cytochrome P450, although the isoforms involved are not well known so far (Zegura et al., 2011; Kittler et al., 2016; Pichardo et al., 2017; Puerto et al., 2018).

Studies performed in vivo in different fish species such as *Oreochromis niloticus*, *Hoplias malabaricus*, and *Poecilia reticulata*, demonstrate that CYN crosses the blood-brain barrier (BBB), probably due to its low molecular weight, as CYN has been linked to tissue damage in the brain after oral and dermal exposure to this cyanotoxin (Guzmán-Guillén et al., 2015; Da Silva et al., 2018; Rabelo et al., 2021). However, to our knowledge, there are no experimental reports regarding neurotoxicity caused by CYN in in vivo mammalian models. However, it has been shown in vitro that CYN may be neurotoxic by causing oxidative stress or changes in the acetylcholinesterase activity (AChE) that might affect synapses (Hinojosa et al., 2019a, 2022). Wang et al. (2020a; b) demonstrated that CYN causes developmental neurotoxicity in zebrafish embryos, being the only study performed in this sense up to now.

Other types of pollutants to be found in different freshwater environments are pesticides, which presence has become an issue in the last decades (Bao et al., 2012; Damalas and Koutroubas, 2016). These chemical compounds aim to protect agricultural products from organisms affecting the crops such as insects or fungal diseases (World Health Organization, 1986; Carvalho, 2017). Around one third of the pesticides used worldwide are organophosphates (OPs), due to their degradability and less persistence in nature compared with other kinds of pesticides (Yang et al., 2005; Singh and Walker, 2006; Dar et al., 2020). From them, the pesticide chlorpyrifos (O,O-diethyl O-3,5,6-trichloropyridin-2-yl phosphorothioate) (CPF) is of specific relevance, which application has led to its detection in edibles and different terrestrial and aquatic environment in many countries (Pengphol et al., 2012; Watts, 2012). Chlorpyrifos affects mainly the nervous system of targeted and non-targeted organisms, which leads to the affectation of other systems such as cardiovascular, endocrine and respiratory might as well (Kavitha and Rao, 2008). This pesticide is oxidized to CPF-oxon by the liver, being approximately 3000 times more potent in terms of toxicity than the main compound (Sultatos, 1991). The main mechanism of action described so far is synaptic disruption due to inhibition of AChE and overstimulation of nAChR and muscarinic acetylcholine receptors (mAChRs) by accumulated acetylcholine (ACh) in the synapses (Alizadeh et al., 2018). Furthermore, CPF has also demonstrated to be able to interact with neurotransmitter receptors and with signal transduction pathways, together with inhibition of macromolecule synthesis, genotoxicity and mutagenicity (Burke et al., 2017; Alizadeh et al., 2018; Rahman et al., 2021). In this sense, the acute exposure to CPF would lead

to the “cholinergic syndrome”, due to the overstimulation of post-synaptic receptors that can have as consequences clinical signs of numbness, dizziness, tremor, nausea, abdominal cramps, sweating, salivation, blurred vision, respiratory depression. After exposure to high doses, unconsciousness, convulsions, and death by respiratory or cardiovascular failure can be observed (Testai et al., 2010). In the case of chronic exposure, the long-term effects of inhibition of AChE in the adult are less defined, although some studies indicate persistent cognitive deficits in a few cases of intoxication (Testai et al., 2010). However, these cholinergic disturbances may have an impact in an immature nervous system, as the brain during its formation is particularly vulnerable compared to the adults (Di Consiglio et al., 2020). This is due to the differences in the BBB permeability and biochemistry during pre- and postnatal brain development (Rodier, 1995; Di Consiglio et al., 2020). In general, the developing nervous system has been reported to be more vulnerable to chemical exposure than the mature one in adults, as disruption on the different processes until its mature formation such as cell proliferation, migration, apoptosis, differentiation, synaptogenesis, myelination, and networking can lead to severe consequences (Bal-Price et al., 2018). In this sense, cholinergic malfunction has demonstrated to cause changes in the adhesion, neurite growth and neural network formation during maturation, as AChE has proven to promote neurite growth in different experimental models (Paraoanu and Layer, 2008). In addition, many studies reviewed by Burke et al. (2017) point out the effects of CPF on developmental neurotoxicity at different stages of gestation, being related to cognitive functions and integrity of the brain structure (Rauh et al., 2012).

As both cyanobacterial compounds and industrial pesticides have been detected in environmental samples such as freshwater or crops, it is relevant to study not only the effects of cyanotoxins isolated but also in combination with other pollutants. In this regard, both compounds have proven to be able to cross the BBB, to affect the nervous system and have demonstrated to exert some damage during development. Thus, the aim of this study was to study the effect of both toxicants, isolated and in combination, in terms of developmental neurotoxicity. For this, the human neuroblastoma SH-SY5Y cell model was used and neuronal differentiation was induced by using all-trans retinoic acid (RA) to measure effects on the neurite outgrowth and viability during 6 days of differentiation. In addition, RA induced neuronal differentiation of SH-SY5Y cells has previously been shown to increase the expression of cholinergic markers e.g. AChE, choline acetyltransferase (ChAT) and nAChR subunits, including the $\alpha 7$ subunit (Loser et al., 2021). To complete those findings, and considering that the main mechanism of action for their neurotoxicity involves disturbed cholinergic signaling, effects on the $\alpha 7$ -subunit homomer nicotinic acetylcholine receptor ($\alpha 7$ -nAChR) induced intracellular Ca^{2+} level were also measured after acute exposure of 3 days differentiated SH-SY5Y cells to the toxicants. Furthermore, a transcriptomic analysis of 93 genes that are differentially expressed in differentiated SH-SY5Y cells and involved in diseases in the nervous system and function were measured using reverse transcriptase (RT)-qPCR after 6 days of differentiation and CYN-exposure, in order to further elucidate a potential developmental neurotoxicity and a possible mechanism thereof.

2. Materials and methods

2.1. Chemicals and reagents

Chlorpyrifos, RA, DMSO, resazurin sodium salt, PNU-120596, sterile water, and FURA 2-AM were purchased from Merck. The cyanotoxin CYN was obtained from Enzo, The MycoAlert Mycoplasma detection Kit was obtained from Lonza. Minimum essential medium (MEM), fetal bovine serum (FBS), L-glutamine, Non-essential amino acid solution (NEAA), streptomycin and penicillin (PenStrep), TrypLE Express Enzyme, Dulbecco's modified Eagle's medium/nutrient mixture F-12 Ham (DMEM/F12), N2 supplements, phosphate buffered saline (PBS),

and poly-D-lysine were purchased from Gibco. Calcein-AM and Hoechst-33342 were obtained from Invitrogen. The RNAeasy Plus Mini Kit was purchased from Qiagen. The iScript cDNA synthesis Kit, PrimePCR DNA contamination control SYBR Green Assay, PrimePCR Reverse Transcription Control SYBR Green Assay, PrimePCR RNA Quality SYBR Green Assay, and SsoAdvanced Universal SYBR Green Supermix were obtained from Bio-Rad. The 75 cm² cell culture flasks, 96-well plates, 60 mm dishes, and black 96-well plates with clear bottom were purchased from Corning. The clear semi-skirted 96-well plates were obtained from Thermo Scientific. The black 96-well plates with μ -clear bottom for fluorescence imaging were from Grainer Bio-One. The polyethersulfone filters were purchased from Sarstedt. The FlexStation II and the black tips were obtained from Molecular Devices. Details can be found in [supplementary table 1 \(ST1\)](#).

2.2. Experimental model and cell culturing

The human neuroblastoma SH-SY5Y cells (passage 55–61) were cultured according to [Attoff et al. \(2016\)](#) and bi-monthly screened for mycoplasma contamination (Lonza MycoAlert Mycoplasma Detection Kit). Briefly, the cells were cultured in complete MEM containing 10% FBS, 1% NEAA, 2 mM L-glutamine and 1% PenStrep (100 U/mL penicillin and 100 μ g/mL streptomycin). For maintenance, the cells were seeded at 10⁵ cells/mL (27000 cells/cm²) in 75 cm² cell culture flasks and incubated in 100% humidity at 37 °C in air with 5% CO₂. The cells were subcultivated every seventh day using 1 mL TrypLE for 2 min at 37 °C. The cells were then differentiated for 3 and 6 days using 1 μ M RA, depending on the experiment ([Attoff et al., 2016](#)). Briefly, after seeding the cells in a 96 well plate for 24 h, the complete MEM was changed to differentiation medium consisting of complete DMEM/F-12 with 1% PenStrep, 2 mM L-glutamine, N2 supplement, and 1 μ M RA (dissolved in ethanol, 0.1% final concentration), with or without the toxics, depending on the experiment.

2.3. Toxic test solutions

Stock solutions of 1 mg/mL CYN and 50 mg/mL CPF were prepared in sterilized milliQ water and DMSO, respectively. Both solutions were maintained at – 20 °C until their use in aliquots to avoid freezing-thawing cycles. The dilution series were freshly prepared in medium or buffer just before exposure to the cells. The concentration of DMSO was adjusted to 0.2% for all concentrations of CPF, CPF in combination with CYN, and the matching negative control. No compensation was made for the addition of milliQ water to medium or buffer in the case of CYN and its negative control.

2.4. Viability

In order to study the effect of CYN and CPF on cell viability, the resazurin assay was performed, according to [O'Brien et al. \(2000\)](#) with some modifications ([Hinojosa et al., 2023](#)). A stock solution of resazurin (880 μ M) was prepared at 20x (weight/volume) by dissolving the resazurin sodium salt in PBS and 0.1 M NaOH, filtered using a 0.22 μ m pore size polyethersulfone filter, and stored at 4 °C protected from light until use. For the viability study, SH-SY5Y cells were seeded in complete MEM at 4 \times 10⁴ cells/mL (12500 cells/cm²) in 100 μ L/well in 96-well clear plates. After 24 h incubation at 37 °C, 5% CO₂ and 100% humidity, the medium was changed to differentiation medium with CYN (0.024–2.4 μ M), CPF (14–570 μ M), and the combination as indicated in [Supplementary Table ST2](#), or without any toxic in the case of the negative controls. After another 72 h incubation, the cells were re-exposed to the toxicants by changing 50 μ L of medium and adding 50 μ L fresh medium including the 2x concentration of the compounds or vehicle and incubated for another 72 h prior to cell viability determination. After 6 days of differentiation and exposure, 50 μ L of medium were removed and 50 μ L of 2x resazurin dissolved in DMEM/F12 were

added. The plates were incubated for 2 h and 30 min, thereafter the resorufin fluorescence was measured at 540 nm excitation and 590 nm emission using a SpectraMax M2 fluorescence reader (Molecular Devices). The experiments were performed in 5 replicates in each experiment, which was repeated 2–9 times, i.e. n = 2–9.

2.5. Neurite outgrowth

For live cell imaging, 4000 cells in 100 μ L/well were seeded in black 96-well plates with μ -clear bottom, precoated with 1 μ g/mL Poly-D-lysine, according to the protocol indicated in [Hinojosa and Johansson et al. \(2023\)](#). The seeding, differentiation and exposure took place under the same conditions used for the viability assessment, but with lower concentrations. Based on the results obtained in the resazurin assay, the concentrations were 0.036–0.48 μ M in the case of CYN, and 14–183 μ M in the case of CPF ([Supplementary Table ST2](#)). The EC₅₀ values obtained for both isolated compounds in the neurite outgrowth assay were used to study the effects of the combination of CYN + CPF in a concentration range from EC₅₀/64 to EC₅₀ in a 1:2 dilution series. After 6 days of differentiation and exposure, cells were loaded with Calcein-AM and Hoechst-33342 to a final concentration in the wells of 1 μ M each. The plates were incubated for 20 min at 37 °C in 5% CO₂ in air, and 130 μ L of DMEM/F12 were added to each well before the fluorescence images were captured by an inverted ZEISS Axio Observer 7 widefield microscope (Carl Zeiss Microscopy GmbH, Jena, Germany) with a Plan-Apochromat 20x/0.8 M27 objective, equipped with an ORCA-Fusion CMOS camera (C15440–200P, Hamamatsu Photonics, Japan). Images were captured in 2 channels using a 405/493/575/654/761 beam splitter. Calcein-AM fluorescence (channel 1, “GFP”) was detected using at ex 488 nm, em 520 nm, while Hoechst-33342 fluorescence was detected at ex 361 nm, em 497 nm for Hoechst (channel 2, “DAPI”), during 50 ms with the ZEN Blue 3.1 software. Six positions per well were depicted by setting manual focus. The images obtained were saved as CZI files. Each experiment was performed in 5 replicates (obtaining 30 images in total per condition and plate), which was repeated 3–4 times (n = 3–4).

Quantitative image analysis was performed using CellProfiler version 3.1.9, using a pipeline that is available on <https://su.drive.sunet.se/index.php/s/chQTKAeifD9WTWD/download>. Neurite outgrowth was defined on a population basis as the ratio of total neurite area to total nuclei area per imaged field. Briefly, the intensity of the neurite pixels was enhanced using the “Speckles” algorithm. The enhanced neurites were subsequently identified as objects based on their size and intensity, setting limits of 5–100. Similarly, nuclei were identified as objects according to their size and intensity, setting a range of 30–300 pixels. Total area occupied by neurite objects was then divided by the total area occupied by nuclei objects in each imaged frame, and the resulting values were used for statistical analysis.

2.6. RNA extraction and cDNA synthesis

SH-SY5Y cells plated in 6 cm in diameter dishes at 12500 cells/cm² in 5 mL medium. After 24 h, the complete MEM was replaced with differentiation medium containing 0.039 μ g/mL (0.097 μ M) CYN, corresponding to EC₂₀ for neurite outgrowth, or just differentiation medium without toxic. After 72 h of exposure, medium was changed by removing half of the medium with fresh 2x CYN diluted in differentiation medium, or just differentiation medium for the control. After 6 days of exposure in total, the medium with or without CYN was removed, and the cells were washed with 5 mL PBS prior detachment with 1 mL TrypLE Express at 37 °C. After 2 min, the cells were resuspended in 4 mL complete MEM medium and centrifuged for 5 min at 300 g. The supernatant was removed and pellets were stored at – 80 °C until RNA extraction. The RNA extraction was performed similarly to in [Hinojosa and Johansson et al. \(2023\)](#), using the RNAeasy Plus Mini kit according to Qiagen's instructions (74134), and a NanoPhotometer P-class spectrophotometer

(Implen GmbH) was used to determine mRNA concentration. Thereafter, 1 µg RNA was reverse transcribed into cDNA using the iScript cDNA synthesis kit from Bio-Rad, and diluted to 10 ng/µL with RNase free water prior to their storage at -80°C . Before performing the RT-qPCR, the quality of the samples was assessed using experimental control assays for genomic DNA, reverse transcription, RNA quality, and PCR performance, all provided by Bio-Rad. The reactions took place in an iQ5 Real-Time PCR Detection System (Bio-Rad) with SsoAdvanced Universal SYBR Green Supermix, also purchased from Bio-Rad. The experiments were performed at 4 separate occasions ($n = 4$).

2.7. Quantitative reverse transcription polymerase chain reaction

The effects of CYN and the control on the 93 selected genes (according to Hinojosa and Johansson et al., 2023) (Supplementary Table S3) were analyzed by RT-qPCR, using pre-casted white 384-well PrimePCR plates with validated primers, designed and purchased (ready to use) from Bio-Rad (<https://www.bio-rad.com/webroot/web/pdf/lsr/global/english/primePCR/LIT10026370.pdf>). For this, 10 ng cDNA in 10 µL were added to each reaction according to the instructions from the provider. On each plate, 2 biological replicates (including the CYN-treated samples and their matching the negative control samples) were added. The reactions were performed using a CFX384 Real-Time PCR Detection System (Bio-Rad) using SsoAdvanced Universal SYBR Green Supermix. The raw data were analyzed using Microsoft Excel. Two housekeeping genes were used for normalization: ribosomal protein large P1 (RPLP1), and heat shock protein 90ab (HSP90AB1). The housekeeping genes selected have previously been identified to be stably expressed (Attoff et al., 2020; Hinojosa and Johansson, 2023). In each sample, the cycle of quantification (Cq) for each gene was subtracted with the mean Cq of the two housekeeping genes (ΔCq). For each gene, the ΔCq of the treated sample was subtracted with the corresponding control ΔCq , labelled as $\Delta\Delta\text{Cq}$. The relative fold change (FC) expression was subsequently calculated by taking 2 to the power of negative $\Delta\Delta\text{Cq}$ ($2^{-\Delta\Delta\text{Cq}}$). The relative fold change expression was then logarithmically scaled (base 2) to give a \log_2 FC value.

2.8. Calcium measurement

Acute changes in the intracellular free calcium levels ($[\text{Ca}^{2+}]_i$), were monitored according to Loser et al. (2021) in order to see the effects of CYN and CPF on the $\alpha 7$ -nAChR activation. Briefly, the SH-SY5Y cells were seeded in complete MEM at 3.5×10^5 cells/mL (109400 cells/cm²) in 100 µL/well in black 96-well plates with clear bottom. After 24 h, the medium was changed to differentiation medium. The cells were incubated for 72 h at 37°C in a humidified atmosphere of 5% CO₂ in air to induce differentiation and expression of $\alpha 7$ -nAChRs. Thereafter, cells were loaded with 4 µM FURA-2AM, dissolved in DMSO (final concentration 0.1%) and diluted in KRH buffer containing NaCl (125 mM), KCl (5 mM), MgSO₄ x 7 H₂O (1.2 mM), KH₂PO₄ (1.2 mM), CaCl₂ x 2 H₂O (2 mM), D-glucose (6 mM) and HEPES (free acid, 25 mM), with pH set to 7.4 with 1 M NaOH. After 30 min of incubation at 37°C , the cells were washed once with 130 µL KRH buffer and then, 90 µL of KRH buffer containing 10 µM of the $\alpha 7$ -nAChRs allosteric modulator N-(5-Chloro-2,4-dimethoxyphenyl)-N'-(5-methyl-3-isoxazolyl)-urea (PNU-120596) were added to the cells. PNU-120596 prevents desensitization by increasing the channel mean open time upon activation but does not interfere with the agonist binding site (Hao et al., 2015). After 20 min of incubation at 37°C , the fluorescence was assessed at 37°C in the fluorescence plate reader FlexStation II (Molecular Devices) at 340 and 380 nm excitation, and 510 nm emission every 4 s using bottom read settings. After 30 s of initial baseline, 10 µL of the toxic were added automatically by the multi-pipette device in the FlexStation II equipment without interruption in the readings, which would lead to 1:10 dilution. In the case of CYN, 0.011–24 µM were added from the compound plate to a final concentration of 0.0011–2.4 µM in 1:3 dilution series in the cell

plate. For CPF, 1.3–2852 µM were added from the compound plate to obtain a final concentration of 0.13–285.2 µM in 1:3 dilution series in the cell plate. The concentrations were prepared in KRH buffer, adding 1% of DMSO to the concentrations of CPF so the final DMSO concentration to the cells was 0.1%. Just KRH was added as negative control for CYN. The fluorescence intensity was monitored for another 210 s after the addition of CYN or CPF. After 240 s in total, 10 µL of 111 µM nicotine were added from the compound plate to the CYN- or CPF- exposed cells and the fluorescence was monitored for 60 s more to assess any inhibitory effect of the toxics on $\alpha 7$ -nAChR activation by an agonist. The change in the Ca²⁺ influx was quantified as area under the curve using the SoftMax Pro 4.8 software (Molecular Devices). The response of the toxics on Ca²⁺ influx was normalized to the response of 11 µM nicotine which was used as a positive control and set to 100%. To estimate the antagonistic effects of CYN and CPF on $\alpha 7$ -nAChR activation, a first addition of KRH buffer and a second addition of 11 µM nicotine (final concentration) were used as positive control.

2.9. Statistical analysis and data storage

Data were presented in relation to control as mean \pm S.D. Number of replicates (n) refer to individual experiments performed at different occasions. Each individual experiment was performed in several technical replicates, except in the RT-qPCR assay. For the curve fit analysis of the cell viability and neurite outgrowth results, the values were normalized, setting 0% as $Y = 0$, and the negative control (cells exposed to only vehicle) to 100%. After this, the concentration-response curve was set as $\log(\text{inhibitor})$ vs. response with variable slope, setting the constants top = 100 and bottom = 0. Statistical analyses were carried out using nonparametric test, not correcting for multiple comparisons, followed by Kruskal-Wallis test in the case of isolated compounds, and by Tukey's multiple comparison tests for the combination, using GraphPad Prism 7. RT-qPCR results were analyzed by comparing the treated ΔCq values with control ΔCq values followed by a paired parametric multiple t-test ($*p < 0.05$). Input data for the heatmaps are presented as \log_2 FC expression in comparison to undifferentiated cells or untreated control cells. The EC values were calculated using the free web calculator from GraphPad Prism by using the EC₅₀ values and the slope factor (<https://www.graphpad.com/quickcalcs/Ecanything1.cfm>). All data were uploaded on <https://su.drive.sunet.se/index.php/s/7XZbkMMbyojgAJw>.

3. Results

3.1. Viability and neurite outgrowth after exposure to CYN or CPF

The effects on cell viability after exposure to CYN during 6 days of differentiation were studied by the resazurin assay (0.024–2.4 µM CYN), while the neurite outgrowth was measured by image analysis of neurons stained with Calcein-AM and Hoechst (0.036–0.48 µM CYN). Both assays demonstrated that CYN caused a concentration-dependent decrease compared to their negative control (non-treated cells) (Fig. 1A). The concentration that caused 50% reduction in the relative number of viable cells (EC₅₀) was set to be the highest concentration used to assess effects on neurite outgrowth, to assure that the effect observed was caused by neurite outgrowth and not by a decrease in cell viability (Table 1).

The effects on viability and neurite outgrowth in SH-SY5Y cells after exposure to CPF during 6 days of differentiation were studied as well (Fig. 1B). In the case of cell viability, CPF tested at 14–570 µM caused a concentration-dependent decrease in cell viability, which was significant after exposure to 171 µM and higher concentrations. The vehicle, DMSO, caused no effects on cellular viability at the concentrations used for CPF dilution (0.2%). Neurite outgrowth was also affected concentration-dependently by CPF (14–183 µM). Non-cytotoxic concentrations of CPF attenuated neurite outgrowth significantly and EC₅₀

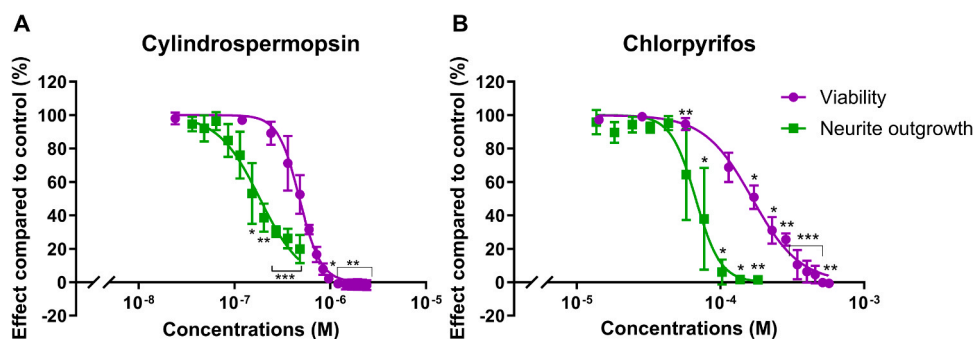


Fig. 1. Effects of CYN and CPF on viability and neurite outgrowth in differentiating SH-SY5Y cells. A) Concentration-effect curves after 6 days treatment of CYN compared to equivalent cells without CYN treatment. Data analyzed using Kruskal-Wallis test. Changes were statistically significant from 0.96 μM for viability ($n = 3-6$) with $p < 0.05$ (*), and $p < 0.01$ (**), and from 0.15 μM for neurite outgrowth ($n = 3$) with $p < 0.05$ (*), $p < 0.01$ (**), and $p < 0.001$ (***) for effects of higher concentrations. B) Concentration-effect curves after 6 days treatment of CPF compared to equivalent cells without CPF treatment. Data analyzed using Kruskal-Wallis test. Changes were statistically significant from 171 μM for viability ($n = 2-5$) with $p < 0.05$ (*), $p < 0.01$ (**), and $p < 0.001$ (***) for effects of higher concentrations, and from 57 μM for neurite outgrowth ($n = 4$) with $p < 0.05$ (*). Data are presented as mean \pm S.D.

Table 1

Estimated EC values for viability and attenuated neurite outgrowth after 6 days of exposure to CYN and CPF during differentiation. Viability data are compared with neurite outgrowth data by using an unpaired t-test. Data are presented as mean \pm S.D., with $p < 0.05$ (*), $p < 0.001$ (***) and $p < 0.0001$ (****).

		EC ₁₀ (μM)	EC ₂₀ (μM)	EC ₅₀ (μM)
CYN	Viability	0.29 \pm 0.06	0.35 \pm 0.06	0.48 \pm 0.05
	Neurite outgrowth	0.066 \pm 0.02	0.097 \pm 0.02 *	0.19 \pm 0.04 *
CPF	Viability	73.7 \pm 17.9	99.5 \pm 18.3	167.6 \pm 14.5
	Neurite outgrowth	52.0 \pm 10.9	57.7 \pm 11.2 *	68.9 \pm 11.7 *

from the viability assessment caused 100% blockage of neurite outgrowth (Fig. 1B; Table 1).

3.2. Viability and neurite outgrowth after exposure to CYN and CPF in combination

In order to see if exposure to the combination of the toxicants enhances or decreases the viability in comparison to the effects of single exposure, the SH-SY5Y cells were exposed for 6 days during differentiation to CYN and CPF in combination in addition to separated exposures. The highest concentrations were EC₅₀ values determined from the viability concentration-effect curves after individual exposure to CYN or

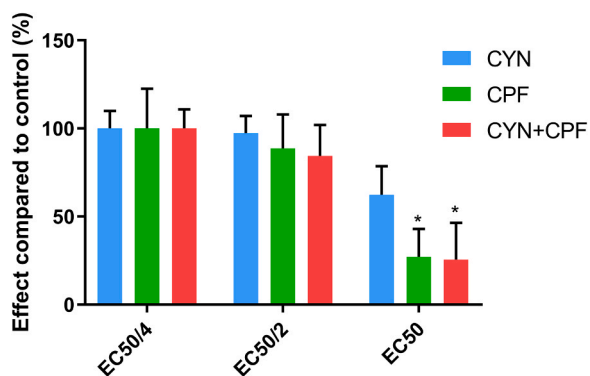


Fig. 2. Effect on viability after exposure to a combination of CYN and CPF compared to the isolated compounds. The cells were exposed to EC₅₀/4 (0.12 μM CYN + 41.9 μM CPF), EC₅₀/2 (0.24 μM CYN + 83.8 μM CPF), and EC₅₀ (0.48 μM CYN + 167.6 μM CPF). Data were analyzed using Tukey's test. Data are presented as mean \pm S.D ($n = 8$). * $p < 0.05$ compared to the equivalent concentration of CYN under the same conditions.

CPF, respectively (Table 1). Thus, the cells were exposed to EC₅₀, EC₅₀/2 and EC₅₀/4 of both compounds (Fig. 2). The results showed a similar response to the combination of CYN and CPF as to the response after exposure to CPF alone.

Neurite outgrowth was assessed after exposure to CYN and CPF in combination, using concentrations that attenuated neurite outgrowth by 50% (EC₅₀) from individual exposures as the highest concentrations for CYN and CPF, respectively. From then, a dilution series of 1:2 was used, which led to a decrease in neurite outgrowth only after exposure to the highest concentrations of exposure. However, when the data were analyzed compared to the results obtained by the isolated toxics, no significant differences were detected between the exposure to the toxics separately in comparison to the exposure to the combination of the compounds (Table 2).

3.3. Effects of CYN on gene expression

SH-SY5Y cells were exposed to EC₂₀ of neurite outgrowth, i.e. 97 nM of CYN during 6 days of differentiation and subsequently harvested for further RT-qPCR analyses of mRNA expression of the selected genes that have been shown to be differentially expressed during differentiation of the cells.

From the statistical analysis it was revealed that CYN significantly downregulated the expression of 5 genes ($p < 0.05$); *NTNG2* (encoding Netrin G2), *KCNJ11* (encoding Potassium Inwardly Rectifying Channel Subfamily J Member 11), *SLC18A3* (encoding Solute Carrier Family 18 Member A3, also called vesicular ACh transporter (vAChT)), *APOE* (encoding Apolipoprotein E), *SEMA6B* (Semaphorin 6B) (Fig. 3).

3.4. Effects of CYN or CPF on intracellular free Ca²⁺ concentration and $\alpha 7$ -nAChR activation

Because CYN exposure decreased mRNA expression of *CHRNA7*

Table 2

Effect on neurite outgrowth of CYN and CPF and the combination of CYN + CPF, being EC₅₀ values 0.19 and 68.9 μM for CYN and CPF, respectively. Data are presented as percentage, mean \pm S.D ($n = 3-6$). No significant variation was detected between each compound after exposure to the same EC.

Concentration (μM)	CYN	CPF	CYN + CPF
EC ₅₀ /64	N/A	N/A	90.6 \pm 5.4
EC ₅₀ /32	N/A	N/A	100.1 \pm 10.7
EC ₅₀ /16	N/A	N/A	90.6 \pm 12.9
EC ₅₀ /8	N/A	N/A	92.4 \pm 7.8
EC ₅₀ /4	93.4 \pm 4.33	100.0 \pm 0.02	84.2 \pm 6.9
EC ₅₀ /2	73.3 \pm 7.9	98.0 \pm 1.2	80.4 \pm 11.6
EC ₅₀	49.5 \pm 8.0	48.1 \pm 28.2	50.6 \pm 19.9

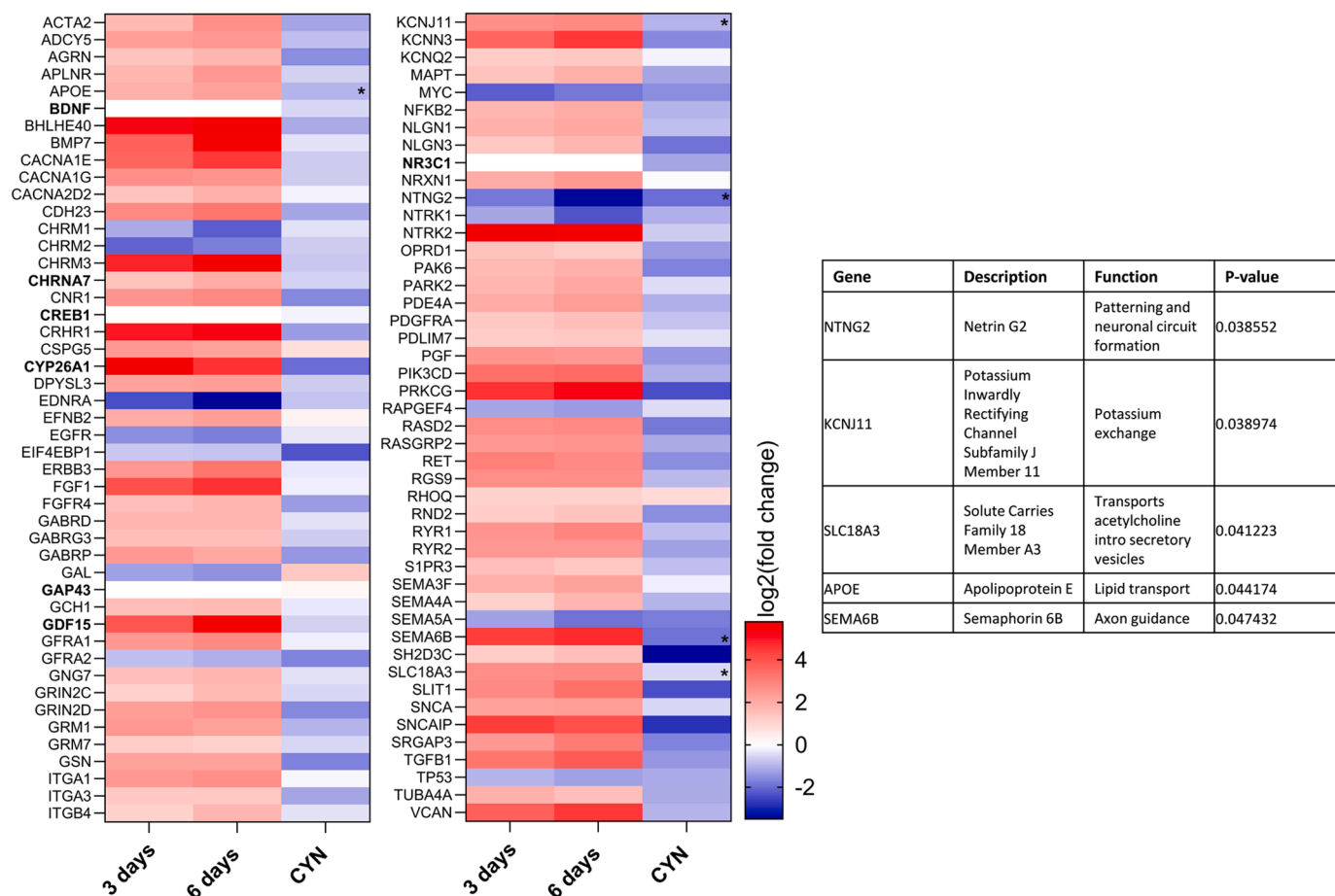


Fig. 3. The effect of CYN on mRNA expression of 93 selected genes in SH-SY5Y cells. Heatmap of the gene expression of genes involved in neuronal development during 3 and 6 days of differentiation (compared to undifferentiated cells – RNA sequencing input data) and following 97 nM CYN exposure during 6 days of differentiation compared to unexposed cells at the same differentiation stage – RT-PCR input data). Data are presented as the mean of 3–4 replicates. Color coding refers to $\log_2(\text{fold change})$. The results were analyzed by paired parametric multiple t-test, * $p < 0.05$. The genes in bold are genes that were selected due to their importance on neurodevelopment.

(however, not statistically significant, $p = 0.075$) and the vAChT-encoding gene *SLC18A3*, we wanted to see if CYN had an acute effect on the $\alpha 7$ -nAChR function. SH-SY5Y cells were differentiated for 3 days and then exposed acutely to 0.0011–2.41 μM CYN (Supplementary Table ST2) in the presence of the $\alpha 7$ -nAChR allosteric modulator PNU-120596. No significant change in the intracellular calcium level $[\text{Ca}^{2+}]_i$ was observed after the addition of CYN in any of the concentrations tested (Fig. 4A). Nicotine (11 μM) was added after the addition of CYN to see if CYN had an antagonistic effect on the $\alpha 7$ -nAChR. The

response of nicotine on Ca^{2+} influx was the same as the one obtained in cells that were pre-exposed to KRH buffer and PNU-120596 (Fig. 4B). Thus, CYN did neither cause any agonistic, nor antagonistic effect on the $\alpha 7$ -nAChR mediated increase in $[\text{Ca}^{2+}]_i$ after acute exposure to concentrations up to 2.4 μM .

For comparison, we also studied the effects of CPF on $[\text{Ca}^{2+}]_i$ and on $\alpha 7$ -nAChR activation. SH-SY5Y cells were exposed acutely to 0.13–285 μM CPF (Supplementary Table ST2) in the presence of PNU-120596 after 3 days of differentiation and the changes in the $[\text{Ca}^{2+}]_i$

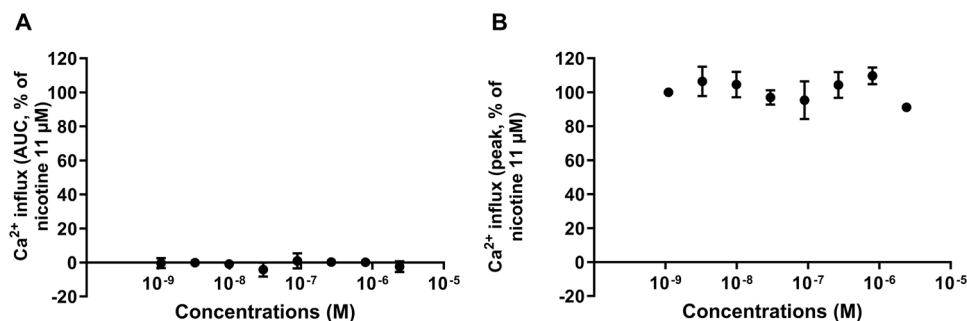


Fig. 4. Acute effects of CYN on the $[\text{Ca}^{2+}]_i$ levels and $\alpha 7$ -nAChR activation in 3-days differentiated SH-SY5Y cells. A) The responses were evaluated as area under the curve (AUC) of the increased fluorescence of Fura-2 for 0–210 s after compound addition. B) The responses were evaluated as peak of the increased fluorescence of Fura-2 for 0–60 s after the addition of 11 μM nicotine. Both responses were normalized to the $[\text{Ca}^{2+}]_i$ response of the cells after depolarization with 11 μM nicotine. Results are shown as mean \pm S.D. ($n = 5$).

were measured, obtaining no significant variation after the addition of CPF in any of the concentrations tested compared to the AUC obtained after exposing to 11 μM nicotine (Fig. 5A). However, 95.1 μM and 285 μM CPF inhibited nicotine induced Ca^{2+} influx significantly, with an estimated IC_{50} value of $83.1 \pm 5.4 \mu\text{M}$ (Fig. 5B). Thus, CPF does not seem to cause any agonistic effect on the $[\text{Ca}^{2+}]_i$, but decreases the response of 11 μM nicotine by modulating the $\alpha 7$ -nAChR activation.

4. Discussion

Diagnoses of neurodevelopmental disturbances have increased in the last decades and understanding the potential role of environmental pollutants is a key for prevention (Lucchini et al., 2017). In this sense, it is important to study the effects of different pollutants on humans, with special attention to the neurotoxic or developmental neurotoxic properties that these compounds could exert. For CYN, the cases of reported human poisoning have been scarce, and not always only due to CYN-exposure. This cyanotoxin is then processed in the body through CYP450-complex and then the metabolites are excreted through urine (Buratti et al., 2017). However, this is an emerging cyanotoxin, and although the human exposure has been prevented through water treatment, this process does not reach the whole population. Despite its already known toxicity in different organs, some studies point out a possible effect of CYN on the nervous system (Yang et al., 2021). Studies concerning its developmental toxicity are also very scarce but relevant (Wang et al., 2020). Thus, the study of this secondary metabolite in terms of finding possible effects on developmental neurotoxicity is of interest. We found that the relative amount of viable SH-SY5Y cells decreased in a concentration-dependent manner after exposure to CYN for 6 days during neuronal differentiation, providing an EC_{50} value of 0.48 μM , but causing significant changes from 0.96 μM . There are no more studies concerning the effects of CYN on nervous cell lines during differentiation. However, some studies have been performed after acute exposure to CYN. In this regard, Hinojosa et al. (2019b), (2023) also measured cell viability in SH-SY5Y cells, but only after exposure for 24 and 48 h, obtaining EC_{50} values of 2.1 μM after 24 h of exposure in undifferentiated cells, and 0.7 μM after 24 h to differentiated cells, demonstrating CYN to be more toxic to the differentiated cells. This might be due to differences in gene expression between the two states of differentiation in the cell line (Attoff et al., 2020). Cytotoxicity studies of CYN have been performed in other cell lines obtained from the nervous system, such as murine microglial BV-2 cells and murine neuroblastoma N2a cells (Takser et al., 2016). They reported a decrease in cell viability after exposure for 24, 48 and 72 h to 0.1 and 10 μM in both cell lines, N2A cells being more sensitive than BV-2 cells. Furthermore, concerning cytotoxicity on murine primary neuronal cultures, exposure to CYN led to a concentration- and time-dependent decrease after exposure to 0.6–2.4 μM CYN during 24 and 48 h (Hinojosa et al., 2022).

Taking the cytotoxicity results of CYN into account, the neurite

outgrowth was measured after exposure during differentiation to non-cytotoxic concentrations. A concentration-dependent decrease in neurite outgrowth was observed from 0.15 μM , leading to an EC_{50} value of 0.19 μM . This is the first time that any effect on this parameter is observed after exposure to CYN. Neurite outgrowth is one of the key processes in the neurodevelopment, and thus, an alteration caused by a toxicant may lead to developmental neurotoxicity (Aschner et al., 2017).

Concerning the effects of CYN on a transcriptomic level, the evaluation of the 93 genes involved in neurodevelopment led to the statistically significant dysregulation of 5 genes. From them, the gene *KCNJ11*, which is coding for an inward rectifying potassium channel subunit of ATP-regulated Kir6.2, was dysregulated. Mutations in *KCNJ11* can cause neurocognitive dysfunction in addition to neonatal diabetes (Landmeier et al., 2017) as well as developmental defects and impaired network excitability in neuronal organoids (Dalgin et al., 2021), indicating that the channel is important for brain development. Another gene that was dysregulated was *APOE*, which is involved in lipid transport and plays an important role in neuronal cell integrity through microtubule and cytoskeleton stabilization. Furthermore, apolipoprotein E is linked to inflammation, atherosclerosis, and Alzheimer's disease and in the differentiation of functional networks in the brain (Raber et al., 2004; Jawien, 2012; Trachtenberg et al., 2012; Nattel et al., 2017). Moreover, CYN exposure led to the dysregulation of *NTNG2*, which is the gene encoding for netrin-G2, which is a protein involved in axonal guidance. Polymorphism variants of netrin-G2 can lead to schizophrenia or bipolar disease, among others (Yaguchi et al., 2014). In addition, dysregulation of *SEMA6B* was also detected, which encodes for a semaphorin, also involved in axonal guidance by the attraction or repulsion of growth cones of developing axons, depending on the subtype (Verhaagen and Pasterkamp, 2009; Alto and Terman, 2017). Hence, dysregulation of these two genes might be involved in the attenuated neurite outgrowth observed after exposure to CYN. Lastly, CYN significantly downregulated *SLC18A3*, which encodes the protein transporting ACh into secretory vesicles (Tie et al., 2022). In this regard, it is also worth to mention that, even if the effect was not statistically significant (p -value = 0.075), *CHRNA7*, the gene encoding the $\alpha 7$ isoform of nAChRs, was also downregulated after the exposure to CYN. To our knowledge, this is the first time that effects of CYN are measured on a transcriptomic level beside studies concerning oxidative stress related gene expression (Pichardo et al., 2017).

Taking these results on gene expression into account, together with the effects observed on neurite outgrowth, led us to study the effects of CYN on nAChR activation. The SH-SY5Y cells express several nAChR subunits which are permeable for Ca^{2+} and, among them, the $\alpha 7$ subunit has demonstrated to be expressed in our cell model after 3 days of differentiation (Loser et al., 2021). Studying the effects on $[\text{Ca}^{2+}]_i$, in particular with respect to these receptors, would give a possible explanation for the results observed in the neurite outgrowth experiments, as neurite outgrowth is a process partly regulated by $[\text{Ca}^{2+}]_i$ (Lankford and

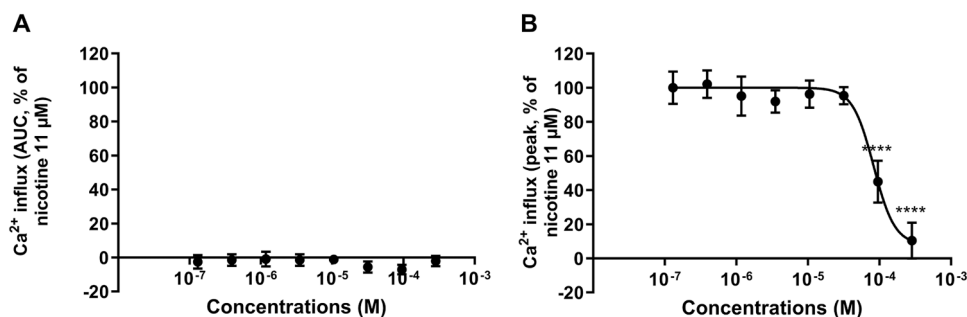


Fig. 5. Acute effects of CPF on the $[\text{Ca}^{2+}]_i$ levels and $\alpha 7$ -nAChR activation in 3-days differentiated SH-SY5Y cells. A) The responses were evaluated as area under the curve (AUC) of the increased fluorescence of Fura-2 for 0–210 s after compound addition. B) The effect of the addition of 11 μM nicotine after pre-exposure to CPF was evaluated as peak of the increased fluorescence of Fura-2 for 0–60 s after the addition of nicotine. * * * * Significantly different from control group ($p < 0.0001$). Both responses were normalized to the $[\text{Ca}^{2+}]_i$ response of the cells after addition of 11 μM nicotine ($n = 5$). Data are presented as mean \pm S.D.

Letourneau, 1991; Takemura et al., 2009). However, CYN does not seem to cause any effect on the $\alpha 7$ -nAChRs in our cell model after acute exposure in 3-days differentiated SH-SY5Y cells, as no significant alterations of $[Ca^{2+}]_i$ levels were detected when exposed to 0.60–2.4 μM CYN compared to the control. In addition, CYN did not affect the response to nicotine after exposure to the same concentrations of CYN. It is important to emphasize that the concentration range used was chosen according to the levels of this toxin found in water supplies under specific circumstances (Yang et al., 2021). Nevertheless, a dysregulation on the gene expression of *CHRNA7* was observed after 6 days of exposure to 97 nM during differentiation, although not statistically different from the control. To our knowledge, there are no studies concerning any effects of this cyanotoxin on AChRs. However, some studies reported alterations on the AChE levels both in vitro and in vivo (Guzmán-Guillén et al., 2015; Da Silva et al., 2018; Hinojosa et al., 2019a; b). Although Hinojosa et al. (2019) did not report any statistically significant alterations after exposure of undifferentiated SH-SY5Y cells to the same concentration range than in the present study, a slight decrease of AChE activity in differentiated cells after exposure to 0.72 μM for 24 h was observed. However, this finding needs to be further studied, as results obtained in fish showed different results. Guzmán-Guillén et al. (2015) reported a decrease in AChE in brain of tilapia fish exposed subchronically to 10 $\mu g/L$ (24 nM) CYN per day for 14 days, while Da Silva et al. (2018) detected an increase of AChE activity after 7 days of exposure to purified CYN in brain in *Hoplias malabaricus* and after 14 days in muscle in the same fish species. However, even though CYN may cause some alteration on AChE, neither agonistic, nor antagonistic effects on the nAChRs seem to be involved in the possible neurotoxic mechanism of action for CYN.

Considering these results and the lack of studies on developmental neurotoxicity caused by CYN, another realistic scenario was combinatory effects of CYN with other pollutants. Among them, the OP-pesticide CPF was an interesting match, due to the effects of these pesticides on developmental neurotoxicity (Burke et al., 2017). Concerning CPF-exposure, the exposure is hard to measure because this pesticide metabolizes quickly in the human body through the CYP450-complex and then is also excreted through urine. The use of this pesticide has been banned from the EU; however, it is still commonly used in different countries around the globe (Wojekko et al., 2022). To study effects of the combination on cell viability and neurite outgrowth, effects of CPF alone on cell viability and neurite outgrowth were also measured for comparison. Concerning the cell viability, CPF caused a concentration-dependent decrease after exposure during 6 days of differentiation, providing an EC_{50} value of 168 μM , with significant decrease in viable cells from 171 μM . These data agree with the results obtained in human induced pluripotent stem cells (hiPSCs)-derived neural progenitors differentiated for 7 days when exposed to CPF for 14 days during differentiation (Pistolato et al., 2020).

Regarding the effects of the OP on neurite outgrowth, the EC_{50} obtained by the resazurin assay was the one chosen as the highest concentration of exposure to assure that the effects perceived by this assay were due to the toxic affecting neurite outgrowth and that its cytotoxic effects were not involved. This assay provided also a concentration-dependent effect with an estimated EC_{50} value of 69 μM , leading to a statistically significant decrease after exposure from 57 μM . Concerning the studies performed in different cell lines, Christen et al. (2017) also reported a decrease of neurite outgrowth in 5 days differentiated rat adrenal gland pheochromocytoma PC12 cells after exposure during differentiation to 9–86 μM , while 171 μM totally inhibited neurite formation. These reports agree with our results, where a concentration-dependent decrease in neurite outgrowth was observed.

No neurite formation was seen at the highest concentrations while viable cells were still present in the cultures. In addition, CPF has demonstrated to cause effects on neurite outgrowth after exposure of human iPSC-derived neurons (Ryan et al., 2016) and of neural stem cells (NSCs) (Di Consiglio et al., 2020). In fact, the study on NSC reported a

concentration-dependent decrease in the number of neurites at non-cytotoxic concentrations after being treated during cell differentiation for 14 days to 18.45–37.10 μM (Di Consiglio et al., 2020). In this sense, neurite outgrowth has demonstrated to be modulated by changes in $[Ca^{2+}]_i$, which is essential for proper neuronal development and function (Meijer et al., 2014a,b). Developmental neurotoxicity has been extensively studied for CPF and is one of the main causes for the recent banning of its use as a pesticide in the European Union (EFSA, 2019). However, the main mechanism of action of CPF is the AChE inhibition. Acute inhibition of AChE leads to accumulation of ACh in the synapse, which can cause enhanced activation of the nAChRs and desensitization (Katz et al., 1997). No effect in the $[Ca^{2+}]_i$ levels was observed in this study after acute exposure of 3 days differentiated SH-SY5Y cells to 0.13–285 μM of CPF in the presence of the $\alpha 7$ -nAChR allosteric modulator. However, after pre-exposure of CPF (from 33.3 μM), the response of the $\alpha 7$ -nAChR agonist nicotine was inhibited, demonstrating that, although CPF is not an agonist of the $\alpha 7$ -nAChRs, it can exert an antagonistic effect of CPF in this subtype of the receptor. However, it has previously been demonstrated that CPF causes an increase in $[Ca^{2+}]_i$ levels in PC12 cells after acute exposure to 10 μM , leading to a concentration-dependent attenuation of depolarization-evoked increase in the $[Ca^{2+}]_i$, with an EC_{50} value of 0.9 μM (Meijer et al., 2014a,b). In addition, Katz et al. (1997) demonstrated that CPF and its metabolite, CPF-oxon, inhibited the binding of a ligand to nAChRs concentration-dependently, providing IC_{50} values of 150 and 5 μM , respectively. Furthermore, preincubation of membranes enriched in heteromeric nAChRs from *Torpedo nobiliana* with the pesticides increased the affinity of the receptor for the ligand (Katz et al., 1997). These results illustrate that CPF and its metabolite may affect intracellular Ca^{2+} homeostasis by several modes of action, where of antagonizing $\alpha 7$ -nAChRs activation is one (Katz et al., 1997).

Concerning longer exposure, Slotkin et al. (2004) studied the effect of CPF in rats after daily subcutaneous injections of 1 mg/kg body weight (bw) on postnatal days 1–4, and after a second exposure to 5 mg/kg bw during postnatal days 11–15. In their study, CPF produced a decrease in the ligand binding affinity to $\alpha 7$ -nAChR in forebrain and cerebellum after exposure during postnatal days 11–15, but did not cause any changes after exposure for 5 nor 10 days. However, they also reported a delayed decrease in ligand binding affinity to the $\alpha 4\beta 2$ -nAChR subtype in the cerebellum on day 10 after exposure on postnatal days 1–5, while no significant changes were observed after the second period of exposure on postnatal days 11–15. These results demonstrate that different nAChR subtypes are affected by CPF and that the timing of exposure during neuronal development is crucial for the targets (Slotkin et al., 2004). This would suggest that CPF can indeed have effects on nAChR which would lead to changes in $[Ca^{2+}]_i$ levels, which could lead to developmental neurotoxic effects, being a possible cause for the observed neurite outgrowth affectation. Considering that the main mechanism of action of CPF is the inhibition of AChE, which would lead to an increase of ACh, these results may occur as a consequence of the overstimulation with ACh and thus, desensitization of the nAChRs (Burke et al., 2017).

When the combination of CYN + CPF was assayed, the concentrations of exposure used for cell viability were the EC_{50} obtained by the toxics isolated, which led to a significant decrease on cell viability after exposure to the highest concentrations. However, when the response of the combination was compared to the one exerted by the toxics alone, no significant differences were detected, not even an additive effect, except for the highest concentrations, compared to the response of CYN alone. This would point out that no increased toxicity was obtained after the exposure of the combination in our experimental model in terms of cell viability. This is contrary to the response obtained by the combination of the same toxics in undifferentiated SH-SY5Y cells after acute exposure for 48 h, as a synergistic response was obtained after exposure to lower concentrations and an antagonistic effect on cell viability was reported after exposure to higher concentrations (Hinojosa et al., 2020).

However, when the same authors performed that experiment after acute exposure for 24 h, an antagonistic effect was obtained after all the concentrations predicted. It is important to mention that the authors measured toxicity after much shorter exposure time and that the ratio in concentration studied was 1:84 for CYN + CPF, while the one used in our study was 1:350 for CYN + CPF. To our knowledge, the previous report by Hinojosa et al. (2020) is the only report available regarding the combination of these two toxicants. Concerning neurite outgrowth, the combination of these toxicants was performed according to the results obtained by CYN and CPF alone in this assay. The mixture led to a significant decrease only after exposure to the mixture of the highest concentrations (0.19 μM + 68.9 μM of CYN + CPF, respectively). This means that the effect of the combination of both toxicants on neurite outgrowth is not enhanced compared to the response caused by the same chemicals isolated.

5. Conclusions

Our study demonstrated that both CYN and CPF caused a concentration-dependent decrease in SH-SY5Y cell viability during differentiation for 6 days. Both toxicants caused a decrease in neurite outgrowth at non-cytotoxic concentrations, indicating adverse neurodevelopment in vitro. In addition, CYN caused dysregulation of 5 genes that are involved in neurodevelopment. Neither CYN, nor CPF had an effect on the $[\text{Ca}^{2+}]_i$ after acute exposure, whereas CPF had an antagonistic effect on $\alpha 7$ -nAChR function, which may be an additional detrimental factor for the developing brain. This is the first time that possible effects of CYN on neurodevelopment are reported. In addition, the combination of both chemicals did not lead to significant interactions, neither in cell viability nor neurite outgrowth. However, the effect of the interaction may vary depending on the concentrations used. Thus, these findings are relevant in order to perform accurate risk assessment of the toxicants, considering realistic scenarios for exposure to combinations of toxicants to humans.

CRedit authorship contribution statement

Hinojosa, M.G.: Conceptualization, Data curation, Formal analysis, Investigation, Methodology, Software, Validation, Visualization, Writing – original draft, reviewing and editing. **Johansson, Y.:** Data curation, Formal analysis, Investigation, Methodology, Software, Writing – review & editing. **Jos, A.:** Writing – review & editing. **Cameán, A.M.:** Writing – review & editing. **Forsby, A.:** Conceptualization, Funding acquisition, Methodology, Project administration, Resources, Supervision, Visualization, Writing – review & editing.

Declaration of Competing Interest

The authors declare that they have no known competing financial interests or personal relationships that could have appeared to influence the work reported in this paper.

Data availability

Data will be made available on request.

Acknowledgments

The authors wish to thank the Swedish fund for research without animal experiment (N2018-0004, F2019-0009 and F2020-0006), the Swedish Research Council (2018-03269), the Ministerio de Economía y Competitividad of Spain (AGL2015-64558-R, MINECO/FEDER, UE) and the Ministerio de Ciencia e Innovación (PID2019-104890RB-I00/AEI/10.13039/501100011033) for the financial support. Furthermore, we would like to thank to Professor Joëlle Rüegg and her group for assisting us to perform RT-qPCR experiments in their laboratory at Uppsala

University.

Appendix A. Supporting information

Supplementary data associated with this article can be found in the online version at doi:10.1016/j.ecoenv.2023.115804.

References

- Alizadeh, R., Rafati, L., Ebrahimi, A.A., Ehrampoush, M.H., Khavidak, S.S., 2018. Chlorpyrifos bioremediation in the environment: a review article. *Environ. Health Sustain. Dev.* 3, 606–615.
- Alto, L.T., Terman, J.R., 2017. Semaphorins and their signaling mechanisms. *Methods Mol. Biol.* 1493, 1–25. https://doi.org/10.1007/978-1-4939-6448-2_1.
- Aschner, M., Ceccatelli, S., Daneshian, M., Fritsche, E., Hasiwa, N., Hartung, T., Hogberg, H.T., Leist, M., Li, A., Mundi, W.R., Padilla, S., Piersma, A.H., Bal-Price, A., Seiler, A., Westerink, R.H., Zimmer, B., Lein, P.J., 2017. Reference compounds for alternative test methods to indicate developmental neurotoxicity (DNT) potential of chemicals: example lists and criteria for their selection and use. *ALTEX* 34, 49–74. <https://doi.org/10.14573/altex.1604201>.
- Attoff, K., Kertika, D., Lundqvist, J., Oredsson, S., Forsby, A., 2016. Acrylamide affects proliferation and differentiation of the neural progenitor cell line C17.2 and the neuroblastoma cell line SH-SY5Y. *Toxicol. Vitro* 35, 100–111. <https://doi.org/10.1016/j.tiv.2016.05.014>.
- Attoff, K., Johansson, Y., Cediel-Ulloa, A., Lundqvist, J., Gupta, R., Caiment, F., Gliga, A., Forsby, A., 2020. Acrylamide alters CREB and retinoic acid signalling pathways during differentiation of the human neuroblastoma SH-SY5Y cell line. *Sci. Rep.* 10, 16714 <https://doi.org/10.1038/s41598-020-73698-6>.
- Bal-Price, A., Pistollato, F., Sachana, M., Bopp, S.K., Munn, S., Worth, A., 2018. Strategies to improve the regulatory assessment of developmental neurotoxicity (DNT) using in vitro methods. *Toxicol. Appl. Pharmacol.* 354, 7–18. <https://doi.org/10.1016/j.taap.2018.02.008>.
- Bao, L.J., Maruya, K.A., Snyder, S.A., Zeng, E.Y., 2012. China's water pollution by persistent organic pollutants. *Environ. Pollut.* 163, 100–108. <https://doi.org/10.1016/j.envpol.2011.12.022>.
- Buratti, F.M., Manganeli, M., Vichi, S., Stefanelli, M., Scardala, S., Testai, E., Funari, E., 2017. Cyanotoxins: producing organisms, occurrence, toxicity, mechanism of action and human health toxicological risk evaluation. *Arch. Toxicol.* 91, 1049–1130. <https://doi.org/10.1007/s00204-016-1913-6>.
- Burke, R.D., Todd, S.W., Lumsden, E., Mullins, R.J., Mamczarz, J., Fawcett, W.P., Gullapalli, R.P., Randall, W.R., Pereira, E.F.R., Albuquerque, E.X., 2017. Developmental neurotoxicity of the organophosphorus insecticide chlorpyrifos: from clinical findings to preclinical models and potential mechanisms. *J. Neurochem.* 142, 162–177. <https://doi.org/10.1111/jnc.14077>.
- Byth, S.Palm, 1980. Island mystery disease. *Med. J. Aust.* 2, 40–42.
- Carvalho, F.P., 2017. Pesticides, environment, and food safety. *Food Energy Secur* 6, 48–60. <https://doi.org/10.1002/fes3.108>.
- Casas-Rodríguez, A., Cameán, A.M., Jos, A., 2022. Potential endocrine disruption of cyanobacterial toxins, microcystins and cylindrospermopsin: a review. *Toxins* 14, 882. <https://doi.org/10.3390/toxins14120882>.
- Christen, V., Rusconi, M., Crettaz, P., Fent, K., 2017. Developmental neurotoxicity of different pesticides in PC-12 cells in vitro. *Toxicol. Appl. Pharmacol.* 325, 25–36. <https://doi.org/10.1016/j.taap.2017.03.027>.
- Da Silva, R.C., Grötzner, S.R., Moura Costa, D.D., Esquivel, J.R., Muelbert, J., Freitas de Magalhães, V., Filipak, F., De Oliveira, C.A., 2018. Comparative bioaccumulation and effects of purified and cellular extract of cylindrospermopsin to freshwater fish *Hoplias malabaricus*. *J. Toxicol. Environ. Health Part A Curr. Issues* 81, 620–632. <https://doi.org/10.1080/15287394.2018.1469101>.
- Dalgin, G., Tryba, A.K., Cohen, A.P., Park, S.Y., Philipson, L.H., Greeley, S.A.W., Garcia 3rd, A.J., 2021. Developmental defects and impaired network excitability in a cerebral organoid model of KCNJ11 p. V59M-related neonatal diabetes. *Sci. Rep.* 11, 21590 <https://doi.org/10.1038/s41598-021-00939-7>.
- Damalás, C.A., Koutroubas, S.D., 2016. Farmers' exposure to pesticides: toxicity types and ways of prevention. *Toxics* 4 (1), 10. <https://doi.org/10.3390/toxics4010001>.
- Dar, M.A., Kaushik, G., Chiu, J.F.V., 2020. Pollution status and biodegradation of organophosphate pesticides in the environment. *Abat. Environ. Pollut.: Trends Strategy*. <https://doi.org/10.1016/B978-0-12-818095-2.00002-3>.
- Di Consiglio, E., Pistollato, F., Mendoza-De Gyves, E., Bal-Price, A., Testai, E., 2020. Integrating biokinetics and in vitro studies to evaluate developmental neurotoxicity induced by chlorpyrifos in human iPSC-derived neural stem cells undergoing differentiation towards neuronal and glial cells. *Reprod. Toxicol.* 98, 174–188. <https://doi.org/10.1016/j.reprotox.2020.09.010>.
- Diez-Quijada, L., Benítez-González, Monte, M., Puerto, M., Jos, A., Cameán, A.M., 2021. Immunotoxic effects induced by microcystins and cylindrospermopsin: a review. *Toxins* 13, 711. <https://doi.org/10.3390/toxins13100711>.
- EFSA, 2019. Statement on the available outcomes of the human health assessment in the context of the pesticides peer review of the active substance chlorpyrifos, 2019 EFSA J. 19, 5809. <https://doi.org/10.2903/j.efsa.2019.5809>.
- Guzmán-Guillén, R., Lomares, I., Moreno, I.M., Prieto, A.I.I., Moyano, R., Blanco, A., Cameán, A.M., 2015. Cylindrospermopsin induces neurotoxicity in tilapia fish (*Oreochromis niloticus*) exposed to *Aphanizomenon ovalisporum*. *Aquat. Toxicol.* 161, 17–24. <https://doi.org/10.1016/j.aquatox.2015.01.024>.

- Hao, Y., Tang, J., Wang, K.W., 2015. Development of automated patch clamp assay for evaluation of $\alpha 7$ nicotinic acetylcholine receptor agonists in automated QPatch-16. *Assay. Drug Dev. Technol.* 13, 174–184. <https://doi.org/10.1089/adt.2014.622>.
- Hinojosa, M.G., Gutiérrez-Praena, D., Prieto, A.I., Guzmán-Guillén, R., Jos, A., Cameán, A.M., 2019a. Neurotoxicity induced by microcystins and cylindrospermopsin: a review. *Sci. Total Environ.* 668, 547–565. <https://doi.org/10.1016/j.scitotenv.2019.02.426>.
- Hinojosa, M.G., Prieto, A.I., Gutiérrez-Praena, D., Moreno, F.J., Cameán, A.M., Jos, A., 2019b. Neurotoxic assessment of microcystin-LR, cylindrospermopsin and their combination on the human neuroblastoma SH-SY5Y cell line. *Chemosphere* 224, 751–764. <https://doi.org/10.1016/j.chemosphere.2019.02.173>.
- Hinojosa, M.G., Prieto, A.I., Gutiérrez-Praena, D., Moreno, F.J., Cameán, A.M., Jos, A., 2020. In vitro assessment of the combination of cylindrospermopsin and the organophosphate chlorpyrifos on the human neuroblastoma SH-SY5Y cell line. *Ecotox. Environ. Saf.* 191, 110222. <https://doi.org/10.1016/j.ecoenv.2020.110222>.
- Hinojosa, M.G., Prieto, A.I., Muñoz-Castro, C., Sánchez-Vico, M.V., Vitorica, J., Cameán, A.M., Jos, Á., 2022. Cytotoxicity and effects on the synapsis induced by pure cylindrospermopsin in an E17 embryonic murine primary neuronal culture in a concentration- and time-dependent manner. *Toxins* 114, 175. <https://doi.org/10.3390/toxins14030175>.
- Hinojosa, M.G., Gutiérrez-Praena, D., López, S., Prieto, A.I., Moreno, F.J., Jos, Á., Cameán, A.M., 2023. Toxic effects of the cylindrospermopsin and chlorpyrifos combination of the differentiated SH-SY5Y human neuroblastoma cell line. *Toxicol.* 227, 107091. <https://doi.org/10.1016/j.toxicol.2023.107091>.
- Hinojosa, M.G., Johansson, Y., Cediel-Ulloa, A., Ivanova, E., Gabring, N., Gliga, A., Forsby, A., 2023. Evaluation of mRNA markers in differentiating human SH-SY5Y cells for estimation of developmental neurotoxicity. *Neurotoxicol.* 18, 65–77. <https://doi.org/10.1016/j.neuro.2023.05.011>.
- Huisman, J., Codd, G.A., Paerl, H.W., Ibelings, B.W., Verspagen, J.M.H., Visser, P.M., 2018. Cyanobacterial blooms. *Nat. Rev. Microbiol.* 16, 471–483. <https://doi.org/10.1038/s41579-018-0040-1>.
- Jawien, J., 2012. The role of an experimental model of atherosclerosis: apoE-knockout mice in developing new drugs against atherosclerosis. *Curr. Pharm. Biotechnol.* 13, 2435–2439. <https://doi.org/10.2174/138920112804583023>.
- Katz, E.J., Cortes, V.I., Eldefrawi, M.E., Eldefrawi, A.T., 1997. Chlorpyrifos, parathion, and their oxons bind to and desensitize a nicotinic acetylcholine receptor: relevance to their toxicities. *Toxicol. Appl. Pharmacol.* 146, 227–236. <https://doi.org/10.1006/taap.1997.8201>.
- Kavitha, P., Rao, J.V., 2008. Toxic effects of chlorpyrifos on antioxidant enzymes and target enzyme acetylcholinesterase interaction in mosquito fish, *Gambusia affinis*. *Environ. Toxicol. Pharmacol.* 26, 192–198. <https://doi.org/10.1016/j.etap.2008.03.010>.
- Kittler, K., Hurtaud-Pessel, D., Maul, R., Kolpre, F., Fessard, V., 2016. In vitro metabolism of the cyanotoxin cylindrospermopsin in HepaRG cells and liver tissue fractions. *Toxicol.* 110, 47–50. <https://doi.org/10.1016/j.toxicol.2015.11.007>.
- Landmeier, K.A., Lanning, M., Carmody, D., Greeley, S.A.W., Msall, M.E., 2017. ADHD, learning difficulties and sleep disturbances associated with KCNJ11-related neonatal diabetes. *Pediatr. Diabetes* 18, 518–523. <https://doi.org/10.1111/pedi.12428>.
- Lankford, K., Letourneau, P., 1991. Role of actin filament and three second-messenger systems in short-term regulation of chick dorsal root ganglion neurite outgrowth. *Cell. Motil. Cytoskeleton.* 20, 7–29. <https://doi.org/10.1002/cm.970200103>.
- Loser, D., Hinojosa, M.G., Blum, J., Schaefer, J., Brüll, M., Johansson, Y., Suciú, I., Grillberger, K., Danker, T., Möller, C., Gardner, I., Ecker, G.F., Bennekou, S.H., Forsby, A., Kraushaar, U., Leist, M., 2021. Functional alterations by a subgroup of neonicotinoid pesticides in human dopaminergic neurons. *Arch. Toxicol.* <https://doi.org/10.1007/s00204-021-03031-1>.
- Lucchini, R., Placidi, D., Cagna, G., Fedrighi, C., Oppini, M., Peli, M., Zoni, S., 2017. Manganese and developmental neurotoxicity. *Adv. Neurobiol.* 18, 13–34. https://doi.org/10.1007/978-3-319-60189-2_2.
- Manning, S.R., Nobles, D.R., 2017. Impact of global warming on water toxicity: cyanotoxins. *Curr. Opin. Food Sci.* 18, 14–20. <https://doi.org/10.1016/j.cofs.2017.09.013>.
- Meijer, M., Dingemans, M.M., van den Berg, M., Westerink, R.H.S., 2014a. Inhibition of voltage-gated calcium channels as common mode of action for (mixtures of) distinct classes of insecticides. *Toxicol. Sci.* 141, 103–111. <https://doi.org/10.1093/toxsci/kfu110>.
- Meijer, M., Hamers, T., Westerink, R.H., 2014b. Acute disturbance of calcium homeostasis in PC12 cells as a novel mechanism of action for (sub)micromolar concentrations of organophosphate insecticides. *Neurotoxicology* 43, 110–116. <https://doi.org/10.1016/j.neuro.2014.01.008>.
- Nattel, S.N., Adrianzen, L., Kessler, E.C., Andelfinger, G., Dehaes, M., Côté-Corriveau, G., Trelles, M.P., 2017. Congenital heart disease and neurodevelopment: clinical manifestations, genetics, mechanisms, and implications. *Can. J. Cardiol.* 33, 1543–1555. <https://doi.org/10.1016/j.cjca.2017.09.020>.
- O'Brien, J., Wilson, I., Orton, T., Pognan, F., 2000. Investigation of the Alamar Blue (resazurin) fluorescent dye for the assessment of mammalian cell cytotoxicity. *Eur. J. Biochem.* 267, 5421–5426. <https://doi.org/10.1046/j.1432-1327.2000.01606.x>.
- Ohtani, I., Moore, R.E., Runnegar, M.T.C., 1992. Cylindrospermopsin: a potent hepatotoxin from the blue-green alga *Cylindrospermopsis raciborskii*. *J. Am. Chem. Soc.* 114, 7941–7942. <https://doi.org/10.1021/ja00046a067>.
- Paroanu, L.E., Layer, P.G., 2008. Acetylcholinesterase in cell adhesion, neurite growth and network formation. *FEBS J.* 275, 618–624. <https://doi.org/10.1111/j.1742-4658.2007.06237.x>.
- Pengphol, S., Uthabutra, J., Arquero, O.A., Nomura, N., Whangchai, K., 2012. Oxidative degradation and detoxification of chlorpyrifos by ultrasonic and ozone treatments. *J. Agric. Sci.* 4, 164. <https://doi.org/10.5539/jas.v4n8p164>.
- Pichardo, S., Cameán, A.M., Jos, Á., 2017. In vitro toxicological assessment of cylindrospermopsin: a review. *Toxins* 9, 402. <https://doi.org/10.3390/toxins9120402>.
- Pistolato, F., De Gyves, E.M., Carpi, D., Bopp, S.K., Nunes, C., Worth, A., Bal-Price, A., 2020. Assessment of developmental neurotoxicity induced by chemical mixtures using an adverse outcome pathway concept. *Environ. Health* 19, 23. <https://doi.org/10.1186/s12940-020-00578-x>.
- Puerto, M., Prieto, A.I., Maisanaba, S., Gutiérrez-Praena, D., Mellado-García, P., Jos, A., Cameán, A.M., 2018. Mutagenic and genotoxic potential of pure cylindrospermopsin by a battery of in vitro tests. *Food Chem. Toxicol.* 121, 413–422. <https://doi.org/10.1016/j.fct.2018.09.013>.
- Rabelo, J.C.S., Hanusch, A.L., De Jesus, L.W.O., Mesquita, L.A., Franco, F.C., Silva, R.A., Sabóia-Morais, S.M.T., 2021. DNA damage induced by cylindrospermopsin on different tissues of the biomonitor fish *Poecilia reticulata*. *Environ. Toxicol.* 1–10. <https://doi.org/10.1002/tox.23111>.
- Raber, J., Huang, Y., Ashford, J.W., 2004. ApoE genotype accounts for the vast majority of AD risk and AD pathology. *Neurobiol. Aging* 25, 641–650. <https://doi.org/10.1016/j.neurobiolaging.2003.12.023>.
- Rahman, H.U.U., Asghar, W., Nazir, W., Sandhu, M.A., Ahmed, A., Khalid, N., 2021. A comprehensive review on chlorpyrifos toxicity with special reference to endocrine disruption: evidence of mechanisms, exposures and mitigation strategies. *Sci. Total Environ.* 755, 142649. <https://doi.org/10.1016/j.scitotenv.2020.142649>.
- Rauh, V.A., Perera, F.P., Horton, M.K., Whyatt, R.M., Bansal, R., Hao, X., Liu, J., Barr, D. B., Slotkin, T.A., Peterson, B.S., 2012. Brain anomalies in children exposed prenatally to a common organophosphate pesticide. *Proc. Natl. Acad. Sci.* 109, 7871–7876. <https://doi.org/10.1073/pnas.1203396109>.
- Rodier, P.M., 1995. Developing brain as a target of toxicity. *Environ. Health Perspect.* 103, 73–76.
- Runnegar, M.T., Kong, S.M., Zhong, Y.Z., Lu, S.C., 1995. Inhibition of reduced glutathione synthesis by cyanobacterial alkaloid cylindrospermopsin in cultured rat hepatocytes. *Biochem Pharmacol.* 49, 219–225. [https://doi.org/10.1016/s0006-2952\(94\)00466-8](https://doi.org/10.1016/s0006-2952(94)00466-8).
- Ryan, K.R., Sirenko, O., Parham, F., Hsieh, J.H., Cromwell, E.F., Tice, R.R., Behl, M., 2016. Neurite outgrowth in human induced pluripotent stem cell-derived neurons as a high-throughput screen for developmental neurotoxicity or neurotoxicity. *Neurotoxicology* 53, 271–281. <https://doi.org/10.1016/j.neuro.2016.02.003>.
- Singh, B.K., Walker, A., 2006. Microbial degradation of organophosphorus compounds, 428e471. *FEMS Microbiol. Rev.* 30. <https://doi.org/10.1111/j.1574-6976.2006.00018.x>.
- Slotkin, T.A., 2004. Cholinergic systems in brain development and disruption by neurotoxicants: nicotine, environmental tobacco smoke, organophosphates. *Toxicol. Appl. Pharmacol.* 198, 132–151. <https://doi.org/10.1016/j.taap.2003.06.001>.
- Sultatos, L.G., 1991. Metabolic activation of the organophosphorus insecticides chlorpyrifos and fenitrothion by perfused rat liver. *Toxicology* 68, 1–9. [https://doi.org/10.1016/0300-483X\(91\)90057-8](https://doi.org/10.1016/0300-483X(91)90057-8).
- Takemura, M., Mishima, T., Wang, Y., Kasahara, J., Fukunaga, K., Ohashi, K., Mizuno, K., 2009. Ca²⁺/calmodulin-dependent protein kinase IV-mediated LIM kinase activation is critical for calcium signal-induced neurite outgrowth. *J. Biol. Chem.* 284, 28554–28562. <https://doi.org/10.1074/jbc.M109.006296>.
- Takser, L., Benachour, N., Husk, B., Cabana, H., Gris, D., 2016. Cyanotoxins at low doses induce apoptosis and inflammatory effects in murine brain cells: potential implications for neurodegenerative diseases. *Toxicol. Rep.* 3, 180–189. <https://doi.org/10.1016/j.toxrep.2015.12.008>.
- Terao, K., Ohmori, S., Igarashi, K., Ohtani, I., Watanabe, M.F., Harada, K.I., Ito, E., Watanabe, M., 1994. Electron-microscopic studies on experimental poisoning in mice induced by cylindrospermopsin isolated from blue-green-alga *Umezakia natans*. *Toxicol.* 32, 833–843. [https://doi.org/10.1016/0041-0101\(94\)90008-6](https://doi.org/10.1016/0041-0101(94)90008-6).
- E. Testai F.M. Buratti E. Di Consiglio Chlorpyrifos Hayes' Handbook of Pesticide Toxicology 2010 doi: 10.1016/B978-0-12-374367-1.00070-7.
- Tie, P., Cheng, J., Xue, M.X., Yin, J., Fu, G., Duan, W.L., 2022. SLC18A3 promoted renal cancer development through acetylcholine/cAMP signaling. *Am. J. Cancer Res.* 12, 4279–4289.
- Trachtenberg, A.J., Filippini, N., Ebmeier, K., Smith, S.M., Karpe, F., Mackay, C., 2012. The effects of APOE on the functional architecture of the resting brain. *NeuroImage* 59, 565–572. <https://doi.org/10.1016/j.neuroimage.2011.07.059>.
- Verhaagen, J., Pasterkamp, R.J., 2009. Semaphorins. *Encycl. Neurosci.* 567–573. <https://doi.org/10.1016/B978-0-08045046-9.00345-4>.
- Wang, L., Chen, G., Xiao, G., Han, L., Wang, Q., Hu, T., 2020a. Cylindrospermopsin induces abnormal vascular development through impairing cytoskeleton and promoting vascular endothelial cell apoptosis by the Rho/ROCK signaling pathway. *Environ. Res.* 183, 109236. <https://doi.org/10.1016/j.envres.2020.109236>.
- Wang, L., Wang, Q., Xiao, G., Chen, G., Han, L., Hu, T., 2020b. Adverse effect of cylindrospermopsin on embryonic development in zebrafish (*Danio rerio*). *Chemosphere* 241, 125060. <https://doi.org/10.1016/j.chemosphere.2019.125060>.
- Watts, M. Chlorpyrifos as a possible global POP. Pesticide Action Network North America, Oakland, CA 2012.
- World Health Organization, United Nations Environment Programme, International Labour Organization, 1986. International Programme on Chemical Safety.. Organophosphorus insecticides: a general introduction. World Health Organization. <https://iris.who.int/handle/10665/40198>.
- Wolejko, E., Łozowicka, B., Jabłońska-Trypuc, A., Pietruszyńska, M., Wydro, U., 2022. Chlorpyrifos occurrence and toxicological risk assessment: a review. *Int. J. Environ. Res. Public Health* 19, 12209. <https://doi.org/10.3390/ijerph191912209>.
- Yaguchi, K., Nishimura-Akiyoshi, S., Kuroki, S., Onodera, T., Itohara, S., 2014. Identification of transcriptional regulatory elements for Ntng1 and Ntng2 genes in mice. *Mol. Brain* 7 (1), 19. <https://doi.org/10.1186/1756-6606-7-19>.

Yang, L., Zhao, Y.H., Zhang, B.X., Yang, C.H., Zhang, X., 2005. Isolation and characterization of a chlorpyrifos and 3,5,6-trichloro-2- pyridinol degrading bacterium, 67e73 FEMS Microbiol. Lett. 251. <https://doi.org/10.1016/j.femsle.2005.07.031>.

Yang, Y., Yu, G., Chen, Y., Jia, N., Li, R., 2021. Four decades of progress in cylindrospermopsin research: the ins and outs of a potent cyanotoxin. J. Hazard. Mater. 406, 124653 <https://doi.org/10.1016/j.jhazmat.2020.124653>.

Žegura, B., Straser, A., Filipič, M., 2011. Genotoxicity and potential carcinogenicity of cyanobacterial toxins – a review. Mutat. Res. 727, 16–41. <https://doi.org/10.1016/j.mrrev.2011.01.002>.